Preprints of the 21st IFAC World Congress (Virtual)
Berlin, Germany, July 12-17, 2020

Model Predictive Control of the AC voltage of an Electric-Vehicle Charging Station with ESS

Dae-Jin Kim *, Young Il Lee**

**Jeju Global Research Center, Korea Institute of Energy Research, Jeju, Korea (e-mail: djk@kier.re.kr)*
*** Seoul National University of Science and Technology, Seoul, Korea (e-mail: yilee@seoultech.ac.kr)*

Abstract: With the recent rapid expansion of electric vehicles, a large number of Electric Vehicle Supply Equipment (EVSE) have been installed. As a result, the impact of EV chargers on the power system is being significantly increased. In particular, the EVSE connected to the distribution network line may act as a peak load, which can adversely affect the voltage stability of the distribution network system when the electric vehicle is quickly charged. In this paper, a Model Predictive Control (MPC) algorithm with disturbance observer (DOB) is proposed for stabilizing voltage of EVs Charging Station which is composed of EV chargers, Photovoltaic (PV), Energy Storage System (ESS) and Loads. The proposed DOB estimate the sum of total current which is the source of voltage fluctuations due to line impedance in the EV charging station. The grid voltage remains stable under the various operating condition including the extreme scenarios by proposed methods. Simulations are performed by means of MATLAB/SIMULINK and result shows the effectiveness of the proposed DOB and MPC control scheme.

Keywords: EV Charging Station, Model Predictive Control, Voltage Control, ESS, EV

1. INTRODUCTION

The EVSE connected to the distribution network line may act as a peak load, which can adversely affect the voltage stability of the distribution network system when the electric vehicle is quickly charged. For this reason, it is necessary to operate the EVSE while maintaining the stability of the power distribution system.

There are studies based on electric vehicle charging pricing strategies to keep the voltage stable in power systems integrated with EVSE [2-3]. First, EV mobility is generated by the travel characteristics of the EV user and predicts the electric vehicle charging load. Then double-layer optimization model which considers both charging cost and voltage deviation was developed to optimize the charging pricing strategy and minimize the total voltage magnitude deviation in the power distribution networks [2]. And a time-of-use (TOU) pricing scheme was proposed and it discussed shifting the EV load demand to off-peak time by the TOU schedule based on EV load demand, residential customer load profile, and service transformer loading constraints [3]. These electric vehicle charging cost strategies do not require additional equipment and are easy to apply. However, the above methods cannot maintain a stable voltage if the instantaneous voltage fluctuation is occurred due to the charging load of the EVSE.

To solve this problem, an DC-link based Electric-Vehicle Charging Station models combined with renewable energy and energy storage system (ESS) and loads as shown in Fig. 1 was introduced in [4-5]. It is an approach to alleviate the charging load of electric vehicle charger connected to power system using energy of ESS and PV. In [4], a decentralized strategy was proposed to control the Medium Voltage DC (MVDC) Bus EV Charging Station. Despite the irregular EV charging

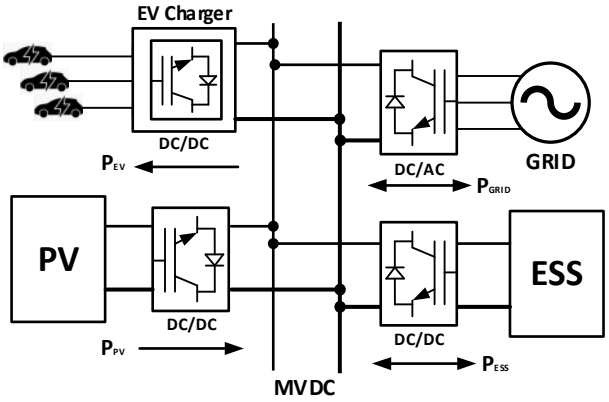

Fig. 1. EV Charging Station with PV and ESS

load, the voltage on the MVDC bus is maintained reliably by PV, ESS with DC/DC converter, and grid-connected three-phase inverters. In this DC link based EV charging station, the EV charger was individually controlled in Constant-Current and Constant-Voltage mode according to the voltage and the optimal power flow scheme was performed [5]. This strategy aims to use the minimum energy from the grid, and EV is considered not only a charging load, but also a source of energy that can be discharged (V2G). The method of operating EV charging stations using the common DC link proposed in these studies is limited to commercial products that meet the operating DC voltage range of the system, thus the flexibility in configuring components of the EV charging station is limited. The inverter-BESS (Battery Energy Storage System) primary control scheme is introduced to support voltage-frequency in AC Microgrids (MG) not only in grid-connected

mode but also in islanded mode [6]. It presented a cascade control type that performs frequency and voltage regulation through Droop control and PI current control. However, since the voltage is controlled by reactive power, it is not suitable for distribution networks with a low X/R ratio. Recently, Artificial Neural Networks (ANN) PI control strategy is proposed to improve the power quality using inverter with BESS in AC MG and it carry out an optimal online tuning of the controller parameters [7].

In this paper, a Model Predictive Control (MPC) algorithm with disturbance observer (DOB) is proposed for stabilizing voltage of EVs Charging Station. The voltage remains stable under the various operating condition including the extreme load condition of the PV, EV and other loads by means of controlling the bi-directional inverter combined with the ESS. In particular, the DOB estimate the total amount of current in the EV charging station, it is not necessary to install additional current sensors and communication lines. A Low Voltage AC (LVAC) of the power distribution system is used to increase the flexibility of component configuration, and the line impedance between the common coupling points of the power distribution system and EV Charging Station is considered.

2. System Description and Modeling

2.1 Bi-directional three phase Inverter with ESS

Fig. 2 shows the topology of three-phase bi-directional inverter with LC filter, where the $V_g^{abc}(V_g^a, V_g^b, V_g^c)$, $V_c^{abc}(V_c^a, V_c^b, V_c^c)$, $V_i^{abc}(V_i^a, V_i^b, V_i^c)$, $i_o^{abc}(i_o^a, i_o^b, i_o^c)$, $i_i^{abc}(i_i^a, i_i^b, i_i^c)$, L_i, C are the three phase grid voltage, output voltage (capacitor voltage), input voltage, inverter output current, inductor current, filter inductors and capacitors respectively. The parasitic resistances are ignored and system parameters are given in Table I. The ESS is connected directly to dc-link of inverter and the voltage of dc-link is varied as the value of state-of-charge (SOC).

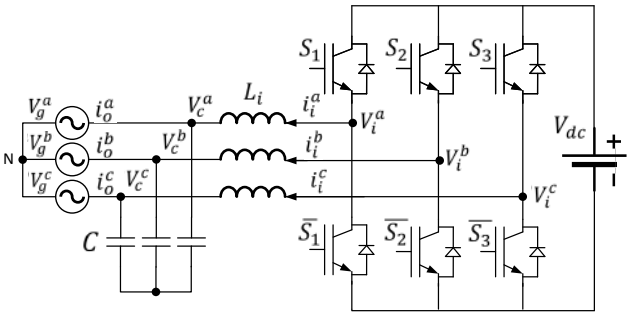

Fig. 2. Three phase grid-connected inverter with LC filter

The switching frequency of the inverter is sufficiently high, so the pulse width modulated elements can be simplified as proportional elements using average switching model. A three-phase system in the stationary frame can be transformed into the synchronous dq frame, and the mathematical model of the LC filter can be represented as follows.

$$\frac{di_i^{dq}}{dt} = wMi_i^{dq} - \frac{1}{L_i}V_c^{dq} + \frac{1}{L_i}V_i^{dq} \tag{1}$$

$$\frac{dV_c^{dq}}{dt} = \frac{1}{C}i_i^{dq} + wMV_c^{dq} - \frac{1}{C}i_o^{dq} \tag{2}$$

where

$$M := \begin{bmatrix} 0 & 1 \\ -1 & 0 \end{bmatrix}$$

The input voltage $V_i^{dq} = [V_i^d \ V_i^q]^{\mathrm{T}}$ are determined by state of the switching devices $S_1 \sim S_3$ including its inverse state $\overline{S_1} \sim \overline{S_3}$ and dc-link voltage V_{dc}. This can be expressed as

$$\begin{bmatrix} V_i^a \\ V_i^b \\ V_i^c \end{bmatrix} = \frac{1}{6}\begin{bmatrix} 2 & -1 & -1 \\ -1 & 2 & -1 \\ -1 & -1 & 2 \end{bmatrix}\begin{bmatrix} S^a \\ S^b \\ S^c \end{bmatrix} V_{dc} \tag{3}$$

where, the S^a, $S^b$and S^c are value of the switching device. In 'ON' state of S_1, the S^a becomes '1' and '0' in the 'OFF' state of S_1. The rest values of S^b and S^c are also determined in the same manner as S^a on the states of the switches S_2 and S_3.

2.2 Distribution Network with Line Impedance

The EV Charging Station is commonly integrated with distribution networks to provide the charging service to customers. In contrast to transmission line, distribution line has low X/R ratio, therefore the voltage of distribution network is sensitive to active power transfer. And thus, the line impedance should be considered in EV Charging Station model as shown in Fig. 3, where L_g, R_g are distribution line reactance and resistance respectively. Assuming that the line impedance is determined in design step of the EV Charging station, it is known parameter.

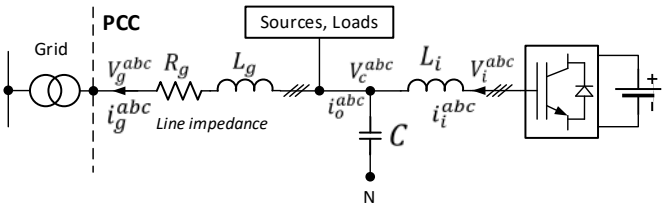

Fig. 3. EV Charging Station with Line Impedance

The line impedance integrated with EV Charging Station can be modeled as

$$\frac{di_g^{dq}}{dt} = \frac{1}{L_g}V_c^{dq} + (wM - \frac{R_g}{L_g})i_g^{dq} - \frac{1}{L_g}V_g^{dq} \tag{4}$$

As it shown in Fig. 3, the i_o^{dq} is the output current of the inverter and output current i_g^{dq} is the total sum of whole component current in EV Charging Station. Defining the disturbance d_g^{dq} caused by the PV, Loads and EV chargers except the inverter, the output current i_g^{dq} can be written as

$$i_g^{dq} := i_o^{dq} + d_g^{dq} \tag{5}$$

Combining (1)-(5), it can be obtained the state-space matrices in (6), including disturbance d_g^{dq} and line impedance R_g and L_g.

The state vector is $\mathbf{x} = [i_i^{dq}\ V_c^{dq}\ i_g^{dq}]^{\mathrm{T}}$ and $\mathbf{u} = [V_i^{dq}]^{\mathrm{T}}$ is control input vector. In addition, two measurements are available in form of output vector $\mathbf{y} = [i_i^{dq}\ V_c^{dq}]$, inductor current i_i^{dq}, capacitor voltage V_c^{dq}, and are expressed as

$$\dot{\mathbf{x}}^{\mathbf{dq}}(\mathrm{t}) = \boldsymbol{A}\mathbf{x}^{\mathbf{dq}}(\mathrm{t}) + \boldsymbol{B}\mathbf{u}^{\mathbf{dq}}(\mathrm{t}) + \boldsymbol{B_c}\mathbf{d}^{\mathbf{dq}}(\mathrm{t}) + \boldsymbol{B_g}\mathbf{V_g}^{\mathbf{dq}}(\mathrm{t}),\ \forall \mathrm{t} \quad (6)$$

$$\mathbf{y}^{\mathbf{dq}}(\mathrm{t}) = \boldsymbol{C}\mathbf{x}^{\mathbf{dq}}(\mathrm{t}),\ \forall \mathrm{t} \quad (7)$$

where

$$\boldsymbol{A} \coloneqq \begin{bmatrix} wM & -\frac{1}{L_i}I_{2\mathrm{x}2} & 0_{2\mathrm{x}2} \\ \frac{1}{C}I_{2\mathrm{x}2} & wM & -\frac{1}{C}I_{2\mathrm{x}2} \\ 0_{2\mathrm{x}2} & \frac{1}{L_g}I_{2\mathrm{x}2} & wM - \frac{R_g}{L_g}I_{2\mathrm{x}2} \end{bmatrix} \boldsymbol{B} \coloneqq \begin{bmatrix} \frac{1}{L_i}I_{2\mathrm{x}2} \\ 0_{2\mathrm{x}2} \\ 0_{2\mathrm{x}2} \end{bmatrix}$$

$$\boldsymbol{B_c} \coloneqq \begin{bmatrix} \frac{1}{L_i}I_{2\mathrm{x}2} \\ I_{2\mathrm{x}2} \\ I_{2\mathrm{x}2} \end{bmatrix} \boldsymbol{B_g} \coloneqq \begin{bmatrix} \frac{1}{L_i}I_{2\mathrm{x}2} \\ I_{2\mathrm{x}2} \\ I_{2\mathrm{x}2} \end{bmatrix} \boldsymbol{C} \coloneqq [I_{4\mathrm{x}4} \quad 0_{2\mathrm{x}2}]$$

The continuous-time space state model in (6)-(7) can be transformed into the following discrete-time space state model with the sampling time T.

$$\mathbf{x}(\mathrm{k}+1) = \mathbf{A}\mathbf{x}(\mathrm{k}) + \mathbf{B}\mathbf{u}(\mathrm{k}) + \mathbf{B_d}\mathbf{d}(\mathrm{k}) + \mathbf{B_g}\mathbf{V_g}(\mathrm{k}),\ \ \forall \mathrm{k} \quad (8)$$

$$\mathbf{y}(\mathrm{k}) = \mathbf{C}\mathbf{x}(\mathrm{t}),\ \forall \mathrm{t} \quad (9)$$

where

$\mathbf{A} \coloneqq e^{AT}, \mathbf{B} \coloneqq \int_0^T e^{A\tau}d\tau \boldsymbol{B_c}, \mathbf{B_d} \coloneqq \int_0^T e^{A\tau}d\tau \boldsymbol{B_d}, \mathbf{B_g} \coloneqq \int_0^T e^{A\tau}d\tau \boldsymbol{B_g}, \mathbf{C} \coloneqq \boldsymbol{C}$.

3. Observer Design

In this section, observer design methods to estimate the state $\mathbf{x}$ and disturbance $\mathbf{d}$ are proposed. The observed state and the observed disturbances are denoted by $\hat{\mathbf{x}}$ and $\hat{\mathbf{d}}$, respectively. The unmeasured value i_g^{dq} is the source of voltage fluctuations due to line impedance. In order to compensate the effect i_g^{dq}, it will be estimated using a disturbance observer.

The discrete-time space state model of (8)-(9) can be expressed follows with the disturbance $\mathbf{d}$

$$\mathbf{d}(\mathrm{k}+1) = \mathbf{d}(\mathrm{k}),\ \ \forall \mathrm{k} \quad (10)$$

$$\mathbf{g}(\mathrm{k}+1) = \mathbf{A_e}\mathbf{g}(\mathrm{k}) + \mathbf{B_e}\mathbf{u}(\mathbf{k}) + \mathbf{B_f}\mathbf{V_g}(\mathrm{k}) \quad (11)$$

$$\mathbf{y}(\mathrm{k}+1) = \mathbf{C_e}\mathbf{g}(\mathrm{k}) \quad (12)$$

Where,

$$\mathbf{g}(\mathbf{k}) \coloneqq \begin{bmatrix} \mathbf{x}(\mathbf{k}) \\ \mathbf{d}(\mathbf{k}) \end{bmatrix}, \mathbf{A_e} \coloneqq \begin{bmatrix} \mathbf{A} & \mathbf{B_d} \\ \mathbf{0_{2x6}} & \mathbf{I_{2x2}} \end{bmatrix}, \mathbf{B_e} \coloneqq \begin{bmatrix} \mathbf{B} \\ \mathbf{0_{4x2}} \end{bmatrix}, \mathbf{B_f} \coloneqq \begin{bmatrix} \mathbf{B_g} \\ \mathbf{0_{4x2}} \end{bmatrix}$$

$$\boldsymbol{C_e} \coloneqq [\mathbf{C}\ \mathbf{0_{4x2}}].$$

In order to verify the observability of the system in (11)-(12), the observability matrix $\mathbf{O}$ is defined as

$$\mathbf{O} \coloneqq [\mathbf{C_e}\ \mathbf{C_eA_e}\ \mathbf{C_eA_e}^2\ \mathbf{C_eA_e}^3]^{\mathbf{T}}.$$

The state observer is constructed to estimates the full state of the inverter model with line impedance. Since this system has two measurements, inductor current i_o^{dq} and capacitor voltage V_c^{dq}, the state observer $\hat{\mathbf{x}}$ can be represented by means of state observer gain $\mathbf{L_1}$ and disturbance observer $\hat{\mathbf{d}}$. The Luenberger type observer is used to make the prediction of state x(k+1) as follows:

$$\hat{\mathbf{x}}(\mathrm{k}+1) = \mathbf{A}\hat{\mathbf{x}}(\mathrm{k}) + \mathbf{B}\mathbf{u}(\mathrm{k}) + \mathbf{L_1}(\mathbf{y} - \mathbf{C}\hat{\mathbf{x}}) + \mathbf{B_d}\hat{\mathbf{d}}(\mathrm{k}) + \mathbf{B_g}\mathbf{V_g}(\mathrm{k}), \quad (13)$$

Where, $\mathbf{V_g}(\mathrm{k})$ is the grid voltage and assumes that the secondary feeder is connected to strong grid, the voltage on PCC is stable condition.

Also, the disturbance observer $\hat{\mathbf{d}}$ can be represented with the disturbance observer gain $\mathbf{L_2}$ and integral action as shown below:

$$\hat{\mathbf{d}}(\mathrm{k}+1) = \hat{\mathbf{d}}(\mathrm{k}) + \mathbf{L_2}(\mathbf{y}(\mathrm{k}) - \hat{\mathbf{y}}(\mathrm{k})),\ \ \forall \mathrm{k} \quad (14)$$

The error of state observer $\mathbf{x}$ and the error of disturbance observer $\mathbf{d}$ are defined as $\tilde{\mathbf{x}}$ and $\tilde{\mathbf{d}}$, respectively, and can be expressed as follows:

$$\tilde{\mathbf{x}}(\mathrm{k}+1) = \mathbf{x}(\mathrm{k}+1) - \hat{\mathbf{x}}(\mathrm{k}+1) \quad (15)$$

$$\tilde{\mathbf{d}}(\mathrm{k}+1) = \mathbf{d}(\mathrm{k}+1) - \hat{\mathbf{d}}(\mathrm{k}+1). \quad (16)$$

Then, substituting (8), (13) into the state observer error in (15) and (10), (14) into the disturbance observer error in (16) yields the augmented state space model as

$$\tilde{\mathbf{g}}(\mathrm{k}+1) = [\mathbf{A_e} - \boldsymbol{L}\mathbf{C_e}]\tilde{\mathbf{g}}(\mathrm{k}) \quad (17)$$

Where,

$$\tilde{\mathbf{g}}(\mathbf{k}) \coloneqq \begin{bmatrix} \tilde{\mathbf{x}}(\mathbf{k}) \\ \tilde{\mathbf{d}}(\mathbf{k}) \end{bmatrix}, \mathbf{L} \coloneqq \begin{bmatrix} \mathbf{L_1} \\ \mathbf{L_2} \end{bmatrix}$$

The system matrix $[\mathbf{A_e} - \mathbf{LC_e}]$ of augmented model should be Hurwitz matrix to converge to zero value of the state observer error and disturbance observer error in (15), (16). In order to determine the observer gain matrix $\mathbf{L}$ of augmented model, suppose that a Lyapunov function defined as

$$\mathrm{V}(\mathrm{k}) = \tilde{\mathbf{g}}(\mathrm{k})\mathbf{P}\tilde{\mathbf{g}}(\mathrm{k}) \quad (18)$$

with $\boldsymbol{P}$ a symmetric positive definite matrix.

$$\mathrm{V}(\mathrm{k}+1) - \mathrm{V}(\mathrm{k}) = \tilde{\mathbf{g}}(\mathrm{k})([\mathbf{A_e} - \mathbf{LC_e}]^{\mathrm{T}}\mathbf{P}[\mathbf{A_e} - \mathbf{LC_e}] - \mathbf{P})\tilde{\mathbf{g}}(\mathrm{k}) < 0 \quad (19)$$

If there exist a symmetric positive definite matrix $\boldsymbol{P}$ in (19), the $[\boldsymbol{A_e} - \boldsymbol{LC_e}]$ is stable and it means the Lyapunov function of (18) is converged to zero with monotonically decreasing. The equation (19) is ensured if

$$\boldsymbol{P} > 0, [\boldsymbol{A_e} - \boldsymbol{LC_e}]^T\boldsymbol{P}[\boldsymbol{A_e} - \boldsymbol{LC_e}] - \boldsymbol{P} < 0 \quad (20)$$

holds. Thus, if there exists the symmetric positive definite matrix $\mathbf{P}$ satisfying (20), the $\mathbf{L}$ is the gain matrix. To guarantee having stability in the sense of Lyapunov:

$$\mathbf{P_o} - [\mathbf{PA_e} - \mathbf{PLC_e}]^{\mathrm{T}}\mathbf{P}^{-1}[\mathbf{PA_e} - \mathbf{PLC_e}] > 0 \quad (21)$$

where, $\mathbf{P_o} > 0$ and $\mathbf{P} > \mathbf{P_o}$.

The inequality (21) can be expressed as a linear matrix inequality (LMI) by applying Schur complement lemma [8]:

$$\begin{bmatrix} \mathbf{P_o} & [\mathbf{PA_e} - \mathbf{YC_e}]^{\mathrm{T}} \\ [\mathbf{PA_e} - \mathbf{YC_e}] & \mathbf{P} \end{bmatrix} > 0 \tag{22}$$

Where, $\mathbf{Y} \coloneqq \mathbf{PL}$.

4. Controller Design

This section presents the design of MPC scheme with full state observer and disturbance observer to regulate the voltage within limits in EV Charging Station. The steady state condition of $\mathbf{x_0}$ satisfy the following:

$$\mathbf{x_0} = \mathbf{Ax_0}(\mathrm{k}) + \mathbf{Bu_0}(\mathrm{k}) + \mathbf{B_d d}(\mathrm{k}) + \mathbf{B_g V_g}(\mathrm{k}) \tag{23}$$

where the $\mathbf{u_0}$ is steady state input. and the disturbance observer error $\tilde{\mathbf{d}}(\mathrm{k})$ will be converge to zero, equation (23) can be represent using the disturbance observer $\hat{\mathbf{d}}(\mathrm{k})$ as:

$$\mathbf{x_0} = \mathbf{Ax_0}(\mathrm{k}) + \mathbf{Bu_0}(\mathrm{k}) + \mathbf{B_d}\hat{\mathbf{d}}(\mathrm{k}) + \mathbf{B_g V_g}(\mathrm{k}) \tag{24}$$

The steady state $\mathbf{x_0}$ can be derived using the reference grid voltage $\mathrm{V_{co}^{dq^*}}$.

$$\begin{aligned} \mathbf{x_0} &= \begin{bmatrix} \mathrm{i_{io}^{dq}} \\ \mathrm{V_{co}^{dq^*}} \\ \mathrm{i_{go}^{dq}} \end{bmatrix} = \begin{bmatrix} \mathrm{A_{11}} & \mathrm{A_{12}} & \mathrm{A_{13}} \\ \mathrm{A_{21}} & \mathrm{A_{22}} & \mathrm{A_{23}} \\ \mathrm{A_{31}} & \mathrm{A_{32}} & \mathrm{A_{33}} \end{bmatrix} \begin{bmatrix} \mathrm{i_{io}^{dq}} \\ \mathrm{V_{co}^{dq^*}} \\ \mathrm{i_{go}^{dq}} \end{bmatrix} \\ &+ \begin{bmatrix} \mathrm{B_{11}} \\ \mathrm{B_{21}} \\ \mathrm{B_{31}} \end{bmatrix} \mathrm{V_{io}^{dq}} + \begin{bmatrix} \mathrm{B_{d1}} \\ \mathrm{B_{d2}} \\ \mathrm{B_{d3}} \end{bmatrix} \hat{\mathbf{d}}^{dq} + \begin{bmatrix} \mathrm{B_{g1}} \\ \mathrm{B_{g2}} \\ \mathrm{B_{g3}} \end{bmatrix} \mathrm{V_g^{dq}} \end{aligned} \tag{25}$$

Where $\mathrm{i_{io}^{dq}}$ and $\mathrm{i_{go}^{dq}}$ are the steady state output current of inverter and sum of total current of EV Charging Station. And $\mathrm{V_{io}^{dq}}$ is the control input of $\mathbf{u_0}$ to inverter in steady state condition.

In order to determine the steady state values of $\mathrm{i_{io}^{dq}}$, $\mathrm{i_{go}^{dq}}$,and the control input $\mathrm{V_{io}^{dq}}$, the state space model of $\mathbf{x_0}$ in (25) will be rearranged as:

$$\begin{bmatrix} i_{io}^{dq} \\ i_{go}^{dq} \\ V_{io}^{dq} \end{bmatrix} = \boldsymbol{G} \begin{bmatrix} A_{12} \\ A_{22} - I_2 \\ A_{32} \end{bmatrix} V_{co}^{dq^*} + \boldsymbol{G} \begin{bmatrix} B_{d1} \\ B_{d2} \\ B_{d3} \end{bmatrix} \hat{\mathbf{d}}^{dq} + \boldsymbol{G} \begin{bmatrix} B_{g1} \\ B_{g2} \\ B_{g3} \end{bmatrix} V_g^{dq} \tag{26}$$

where

$$\boldsymbol{G} \coloneqq \begin{bmatrix} I_{2\mathrm{x}2} - \mathrm{A_{11}} & -\mathrm{A_{13}} & -\mathrm{B_{11}} \\ -\mathrm{A_{21}} & -\mathrm{A_{23}} & -\mathrm{B_{12}} \\ -\mathrm{A_{31}} & I_{2\mathrm{x}2} - \mathrm{A_{33}} & -\mathrm{B_{13}} \end{bmatrix}^{-1}$$

The one-step ahead prediction error state $\hat{\mathbf{e}}(\mathrm{k}+1)$ to steady state can be defined as:

$$\begin{aligned} \hat{\mathbf{e}}(\mathrm{k}+1) &= \hat{\mathbf{x}}(\mathrm{k}+1) - \mathbf{x_0}(\mathrm{k}) \\ &= \mathbf{A}\hat{\mathbf{x}}(\mathrm{k}) + \mathbf{Bu}(\mathrm{k}) + \mathbf{L_1}(\mathbf{y} - \mathbf{C}\hat{\mathbf{x}}) - \mathbf{Ax_0}(\mathrm{k}) - \mathbf{Bu_0}(\mathrm{k}) \end{aligned} \tag{27}$$

A cost index is defined in (28) to minimize the estimated state error against steady state $\mathbf{x_0}$ and penalize the control input to steady state input $\mathbf{u_0}$. Therefore, it is optimization problem as presented in (29).

$$\mathrm{J}\big(\hat{\mathbf{x}}(\mathrm{k}), \mathbf{u}(\mathrm{k})\big) \coloneqq \|\hat{\mathbf{e}}(\mathrm{k}+1)\|_{\mathrm{P}} + \|\mathbf{u}(\mathrm{k}) - \mathbf{u_0}(\mathrm{k})\|_{\mathrm{R}} \tag{28}$$

$$\min_{\mathrm{u(k)}} \mathrm{J}\big(\hat{\mathbf{x}}(\mathrm{k}), \mathbf{u}(\mathrm{k})\big) \tag{29}$$

where, $\mathbf{P}$ is error state cost weight matrix and $\mathbf{R}$ is error input weight matrix.

Then, the cost index is derived as followed.

$$\begin{aligned} &\mathrm{J}\big(\hat{\mathbf{x}}(\mathbf{k}), \mathbf{u}(\mathbf{k})\big) = \|\mathbf{w}(\mathbf{k})\|_{\mathrm{P}} + \|\mathbf{Bu}(\mathbf{k})\|_{\mathrm{P}} + \\ &2\mathbf{u}^{\mathrm{T}}(\mathrm{k})\mathbf{B}^{\mathrm{T}}\mathbf{P}\mathbf{w}(\mathrm{k}) + \|\mathbf{u}(\mathrm{k}) - \mathbf{u_0}(\mathrm{k})\|_{\mathrm{R}} \\ &= \mathbf{w}^{\mathrm{T}}(\mathrm{k})\mathbf{P}\mathbf{w}(\mathrm{k}) + \mathbf{u}^{\mathrm{T}}(\mathrm{k})(\mathbf{B}^{\mathrm{T}}\mathbf{P}\mathbf{B}(\mathrm{k}) + \mathbf{R})\mathbf{u}(\mathrm{k}) \\ &+ 2\mathbf{u}^{\mathrm{T}}(\mathrm{k})\big(\mathbf{B}^{\mathrm{T}}\mathbf{P}\mathbf{w}(\mathrm{k}) - \mathbf{R}\mathbf{u_0}(\mathrm{k})\big) + \mathbf{R}\mathbf{u}_0^2(\mathrm{k}) \end{aligned} \tag{30}$$

where $\mathbf{w}(\mathrm{k}) \coloneqq \mathbf{A}\hat{\mathbf{x}}(\mathrm{k}) + \mathbf{L_1}(\mathbf{y}(\mathrm{k}) - \mathbf{C}\hat{\mathbf{x}}(\mathrm{k})) - \mathbf{Ax_0}(\mathrm{k}) - \mathbf{Bu_0}(\mathrm{k})$.

Therefore, the proposed MPC scheme with disturbance observer is configured as shown in Fig. 3.

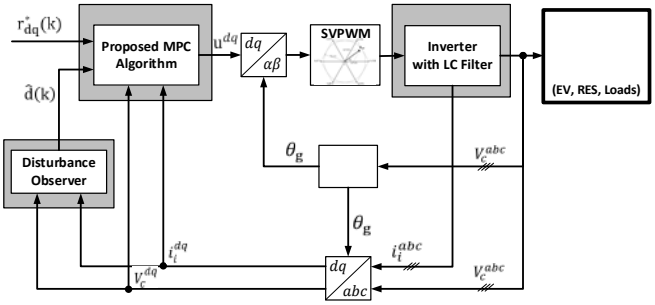

Fig. 3. Block diagram of proposed control scheme

The cost index has a convex form and the input u can be determined by the following equation [9].

$$\frac{\partial \mathrm{J}(\hat{\mathbf{x}}(\mathrm{k}),\ \mathbf{u}(\mathrm{k}))}{\partial \mathbf{u}} = 0,\ \forall \mathrm{k} \tag{31}$$

$$\begin{aligned} \mathbf{u}(\mathrm{k}) &= -(\mathbf{B}^{\mathrm{T}}\mathbf{P}\mathbf{B} + \mathbf{R})^{-1}(\mathbf{B}^{\mathrm{T}}\mathbf{P}\mathbf{w}(\mathrm{k}) - \mathbf{R}\mathbf{u_0}(\mathrm{k})) \\ &= \mathbf{M}\mathbf{B}^{\mathbf{T}}\mathbf{P}\mathbf{A}\hat{\mathbf{e}}(\mathrm{k}) - (\mathbf{M}\mathbf{B}^{\mathbf{T}}\mathbf{P}\mathbf{B} + \mathbf{M}\mathbf{R})\mathbf{u_0}(\mathrm{k}) \\ &+ \mathbf{M}\mathbf{B}^{\mathbf{T}}\mathbf{P}\mathbf{L_1}(\mathbf{y}(\mathrm{k}) - \mathbf{C}\hat{\mathbf{x}}(\mathrm{k})) \end{aligned} \tag{32}$$

where, $\mathbf{M} \coloneqq -(\mathbf{B}^{\mathbf{T}}\mathbf{P}\mathbf{B} + \mathbf{R})^{-1}$

Here, the weight matrices P and Q should be satisfying the stability of the system as control input in (27). Let assume that the P and R are satisfied as follows:

$$\mathbf{B}^{\mathbf{T}}\mathbf{P}\mathbf{B} = \alpha\mathbf{I_2} \tag{33}$$

$$\mathbf{R} = \beta\mathbf{I_2} \tag{34}$$

The above equation (32) can be express as:

$$\Delta\mathbf{u}(\mathrm{k}) = \mathbf{M}\mathbf{B}^{\mathbf{T}}\mathbf{P}\mathbf{A}\hat{\mathbf{e}}(\mathrm{k}) + \mathbf{M}\mathbf{B}^{\mathbf{T}}\mathbf{P}\mathbf{L_1}\big(\mathbf{y}(\mathrm{k}) - \mathbf{C}\hat{\mathbf{x}}(\mathrm{k})\big) \tag{35}$$

where, $\Delta\mathbf{u}(\mathrm{k}) \coloneqq \mathbf{u}(\mathrm{k}) - \mathbf{u_0}(\mathrm{k})$ and $\mathbf{M} \coloneqq -(\alpha + \beta)^{-1}\mathbf{I_2}$ which is redefined using assumption (28) and (29), respectively.

In the case of state observer $\hat{\mathbf{x}}(k)$ follows state $\mathbf{x}(k)$ while satisfying equation (36), the above equation can be represented as:

$$|\mathbf{x}(k) - \hat{\mathbf{x}}(k)| \approx 0 \quad (36)$$

$$\Delta\mathbf{u}(k) = \mathbf{K}\hat{\mathbf{e}}(k) \quad (37)$$

where, $\mathbf{K} \coloneqq \mathbf{M}\mathbf{B}^{T}\mathbf{P}\mathbf{A}$.

The cost function defined in (28) should be monotonically decreasing to satisfy Lyapunov stability as:

$$\begin{aligned} &J(k) - J(k-1) \\ &= \hat{\mathbf{e}}(k)^{T}[(\mathbf{A}+\mathbf{B}\mathbf{K})^{T}\mathbf{P}(\mathbf{A}+\mathbf{B}\mathbf{K}) + \mathbf{K}^{T}\mathbf{R}\mathbf{K}]\hat{\mathbf{e}}(k) \\ &- \{\hat{\mathbf{e}}(k)^{T}\mathbf{P}\hat{\mathbf{e}}(k) + \Delta\mathbf{u}(k-1)^{T}\mathbf{R}\Delta\mathbf{u}(k-1)\} \\ &= \hat{\mathbf{e}}(k)^{T}[(\mathbf{A}+\mathbf{B}\mathbf{K})^{T}\mathbf{P}(\mathbf{A}+\mathbf{B}\mathbf{K}) + \mathbf{K}^{T}\mathbf{R}\mathbf{K} - \mathbf{P}]\hat{\mathbf{e}}(k) - \\ &\Delta\mathbf{u}(k-1)^{T}\mathbf{R}\Delta\mathbf{u}(k-1) < 0 \end{aligned} \quad (38)$$

Since $\Delta\mathbf{u}(k-1)^{T}\mathbf{R}\Delta\mathbf{u}(k-1)$ in equation (38) always has a positive value, it can be rewritten as follows:

$$\hat{\mathbf{e}}(k)^{T}[(\mathbf{A}+\mathbf{B}\mathbf{K})^{T}\mathbf{P}(\mathbf{A}+\mathbf{B}\mathbf{K}) + \mathbf{K}^{T}\mathbf{R}\mathbf{K} - \mathbf{P}]\hat{\mathbf{e}}(k) < 0 \quad (39)$$

The equation (39) is ensured if

$$\mathbf{P} - (\mathbf{A}+\mathbf{B}\mathbf{K})^{T}\mathbf{P}(\mathbf{A}+\mathbf{B}\mathbf{K}) - \mathbf{K}^{T}\mathbf{R}\mathbf{K} > 0 \quad (40)$$

holds, $\mathbf{K}$ is a stabilizing gain matrix if there exists a positive definite matrix P which is satisfying (40). By multiplying Q ($\coloneqq P^{-1}$) on the left- and right-hand sides of (40) and applying Schur complement lemma [8], we obtain

$$\begin{bmatrix} \mathbf{Q} - \mathbf{Y}^{T}\mathbf{R}\mathbf{Y} & [\mathbf{A}\mathbf{Q}+\mathbf{B}\mathbf{Y}]^{T} \\ [\mathbf{A}\mathbf{Q}+\mathbf{B}\mathbf{Y}] & \mathbf{Q} \end{bmatrix} > 0, \mathbf{Q} > 0 \quad (41)$$

where, $\mathbf{Y} \coloneqq \mathbf{K}\mathbf{Q}$.

Since $\mathbf{R}$ is positive definite, it can be assumed that

$$\alpha\mathbf{Q} = \mathbf{Q_o} \ \ (0 < \alpha < 1) \quad (42)$$

where, α is design parameter.

Finally, LMI problem presented in Equation (43) can be represented as:

$$\begin{bmatrix} \mathbf{Q_o} & [\mathbf{A}\mathbf{Q}+\mathbf{B}\mathbf{Y}]^{T} \\ [\mathbf{A}\mathbf{Q}+\mathbf{B}\mathbf{Y}] & \mathbf{Q} \end{bmatrix} > 0. \quad (43)$$

5. Simulation Result

In this section, the simulation result is presented to compare the performance of proposed algorithm against conventional PI controller using MATLAB/SIMULINK. And the EV Charging Station used for the simulation consists of EV Charger, PV, ESS, and the detailed parameters are shown in Table 1 below.

Table 1
SYSTEM PAREMETERS

Symbol	Description	Value
V_g^{abc}	Grid voltage (Phase-Neutral)	220V
f_g	Grid frequency	60Hz
V_{dc}	DC-link voltage (Nominal)	600V
L_i^{abc}	Inverter side inductance	10mH
C^{abc}	Filter capacitance	0.1uF
T	Switching time	100us
R_g, L_g	Line impedance R, L	0.35 ohm 0.1 mH

Fig. 4 shows the simulation result of proposed controller and conventional PI controller. The AC voltage measured at the EV charging station fluctuates by a rapid EV charging load in 0.2 seconds and Photovoltaic power generation in 0.4 seconds. As it can see the grid voltage recovers to nominal voltage in a short time, the transient behavior of the proposed MPC controller is better performance than the PI controller

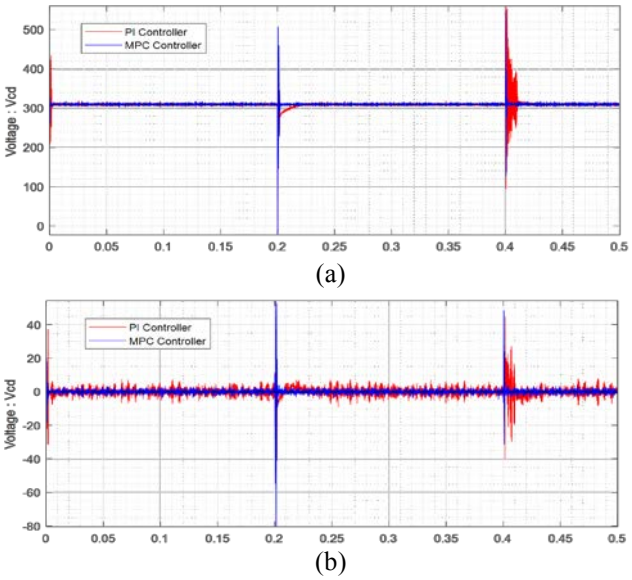

(a)
(b)

Fig. 4. Comparison data of simulation result in dq-axis grid voltage with proposed MPC and PI. (a) grid voltage in d-axis. (b) grid voltage in q-axis.

The transient response of the both controllers is represented in ABC three phase system. In Fig. 5. (a), the black line indicates three phase voltage in case of no load condition and red line means the voltage which shows EV charging load injected grid with PI controller. Under the same conditions as above, (b) shows the result of the voltage to which MPC was applied. Obviously, this simulation results presents that the voltage of EV Charging Station with proposed MPC algorithm is stabilized quickly.

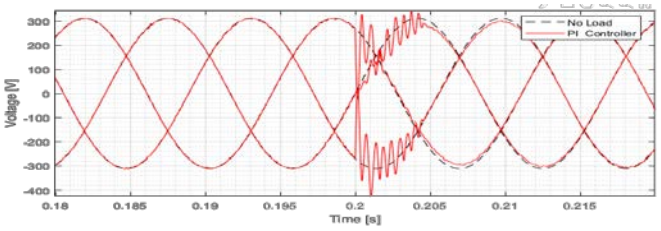

(a)

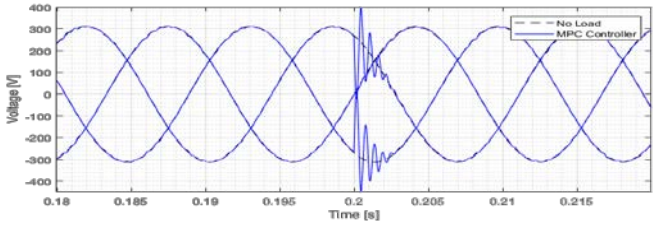

(b)

Fig. 5. Simulation result of no load condition and EV load condition in ABC grid voltage coordinate system (a) No load condition (dotted line) and EV load with PI Controller (red line) (b) No load condition (dotted line) and EV load with proposed MPC Controller (blue line)

Fig. 6 shows the voltage fluctuations caused by PV power generation with an electric current flow opposite to the EV Charging load. In (a) and (b) of Fig. 6, the dotted line represents the ideal voltage of three phases when there is no load condition, and the red and blue lines represent the results of voltage control by the PI Controller and proposed MPC, respectively.

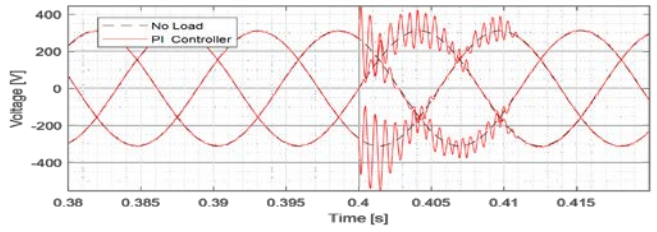

(a)

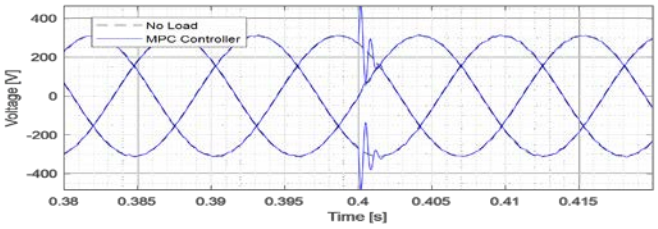

(b)

Fig. 6. Simulation result of no load condition and PV power generation condition in ABC grid voltage coordinate system (a) No load condition (dotted line) and PV power generation with PI Controller (red line) (b) No load condition (dotted line) and PV power generation with proposed MPC Controller (blue line)

6. Conclusion

This study proposed a model predictive control to stabilize the grid voltage in EV Charging Station within limits while the EV charging loads are activated. This control scheme is based on regulating the amount of total current, which is estimated by the disturbance observer. A Lyapunov stability was used to determine the estimation gain matrix by means of LMI method. The improvement of proposed algorithm compared to conventional algorithm has been demonstrated through the simulation in MATLAB/SIMULINK. The proposed control scheme provides stable operation of EV Charging Station without an additional device to measure total current. The simulation shows that the proposed scheme provides the stable voltage under EV Charging condition and is able to adapt to practical applications.

ACKNOWLEDGEMENTS

This research was supported partly by Basic Science Research Program through the National Research Foundation of Korea(NRF) funded by the Ministry of Education(NRF-2019R1A6A1A03032119) and conducted partly by the Ministry of Trade, Industry & Energy(MOTIE), Korea Institute for Advancement of Technology(KIAT) with the support of Chungbuk institute for regional program evaluation as an Encouragement Program for The Industries of Economic Cooperation Region (P0004679).

REFERENCES

[1] William Visser, “Electric vehicle charging - Definitions and explanation”, Netherlands Enterprise Agency, January 2019

[2] X. Dong, Y. Mu, X. Xu, H. Jia, J. Wu, X. Yu, Yan Qi, "A charging pricing strategy of electric vehicle fast charging stations for the voltage control of electricity distribution networks", Applied Energy, Volume 225, Pages 857-868, 2018.

[3] A. Dubey, S. Santoso, M. P. Cloud, and M. Waclawiak, ‘‘Determining timeof-use schedules for electric vehicle loads: A practical perspective,’’ IEEE Power Energy Technol. Syst. J., vol. 2, no. 1, pp. 12–20, Mar. 2015.

[4] P. García-Triviño, J. P. Torreglosa, L. M. Fernández-Ramírez, F. Jurado, "Control and operation of power sources in a medium-voltage direct-current microgrid for an electric vehicle fast charging station with a photovoltaic and a battery energy storage system", Energy, Volume 115, Part 1, Pages 38-48, 2016.

[5] W. Khan, F. Ahmad, M. Saad Alam, "Fast EV charging station integration with grid ensuring optimal and quality power exchange", Engineering Science and Technology, an International Journal, Volume 22, Issue 1, Pages 143-152, 2019.

[6] Fusero, M.; Tuckey, A.; Rosini, A.; Serra, P.; Procopio, R.; Bonfiglio, A. A Comprehensive Inverter-BESS Primary Control for AC Microgrids. Energies 2019, 12, 3810.

[7] Alshehri, J.; Khalid, M.; Alzahrani, A. An Intelligent Battery Energy Storage-Based Controller for Power Quality Improvement in Microgrids. *Energies* 2019, *12*, 2112.

[8] S. P. Boyd, L. E. Ghaoui, E. Feron, and V. Balakrishnan, Linear Matrix Inequalities in System and Control Theory. Philadelphia, PA, USA: SIAM, 1994.

[9] Kim S.K., Park C.R., Yoon T.W., Lee Y.I, Disturbance-observer-based model predictive control for output voltage regulation of three-phase inverter for uninterruptible-power-supply applications, European Journal of Control, Volume 23, Pages 71-83, 2015.